**Contemporary Engineering Sciences, Vol. 10, 2017, no. 21, 1035 - 1046**
**HIKARI Ltd, www.m-hikari.com**
**https://doi.org/10.12988/ces.2017.79112**

# Locating Distributed Generation Units in Radial Systems

**Gabriel González Palomino**

Universidad Autónoma de Occidente, Colombia

**Luis Alejandro Arias Barragán**

Universidad Autónoma De Colombia, Colombia

**Edwin Rivas Trujillo**

Universidad Distrital francisco José de Caldas, Colombia



**Abstract**

A brief context on distributed generation (DG) is given as well as the methodologies employed in solving problems regarding their optimal location and dimensioning in electrical power systems that sets the theoretical foundation of this project. The development of a Python-based analytical algorithm is shown which interacts with the DigSilent software for the optimal management of distributed generation units in terms of their dimension and location in radial systems. The proposed algorithm is based on the formulation in the analytical method of location and dimensioning of DG units in distribution systems [1] with a 33-node IEEE radial system used a case study.

The implementation of the algorithm justifies that the optimal location of DG units in electrical radial systems improves the voltage profiles and the reduction of total losses.

**Keywords**: Distributed Generation, Optimization, Radial Systems

# 1 Introduction

Distributed or decentralized generation is a fundamental part of the Smart City and consists on the generation of electrical energy through a variety of small generation sources installed near the end users [2] [3] [4]. Distributed generation is a cooperation system between micro-generation and the generation of conventional stations. This distribution offers a more balanced generation and lets the Smart City not so dependent on the big stations. Additionally, micro-generation implies the use of renewable energies which will reduce the $CO_2$ emissions [4]. This generation presents various advantages for electrical systems such as the improvement on voltage profile, reliability and security of the system, reduction of losses and solving congestion [4]. Hence, there is a great interest in proposing strategies that can find the best location of the DG units plus adequately injecting power in the electrical systems with the purpose of avoiding over-dimensioning and minimizing costs.

In scientific literature, diverse methodologies have been used to find the location of DG units in electrical systems so it is important to adopt methods that optimally assign from the demand stand point as well as considering the places and the DG system's differential capacities [5] [6].

The present article is organized as follows: In section I, the introduction focuses on the concept of DG and some strategies implemented in solving the problem of dimensioning and locating DG units in electrical power systems; in section II, the testing radial system used as a case study is shown indicating the parameters of impedances and active/reactive power for each node; in section III, the method used for dimensioning is detailed and it is based on the calculation of effective power and the losses associated with the nodes; in section IV, the methodology implemented is described as well as the algorithm developed with the PYTHON and DIGSILENT software; in section V, the results obtained with the testing network are shown in terms of the losses and the voltage profiles in the nodes; in section VI, the results are analyzed; and finally some conclusions are provided on the overall work.

## 2 33-Node IEEE Radial System for Testing

The proposed electrical system used as a case study is shown in Figure 1. It is a radial network with 33 nodes.

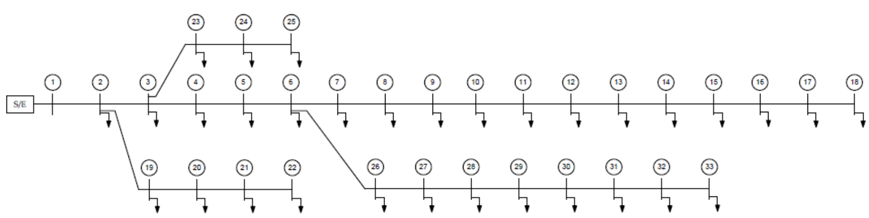


**Figure 1.** 33-node IEEE radial network topology.

The voltage level of the substation connected to the bus n° 1 is 12.66 kV with a peak load of 3.72 MW and 2.30 MVAR for an apparent power of 4.37 MVA. The system's active power loss is 0.202 MW, the reactive power losses correspond to 0.134 MVAR [7].

To set the system's configuration the data from Table 1 are taken. The impedances are in ohm, the loads in MW and MVAR respectively, $P_L$ and $Q_L$ are the active and reactive power connected to the respective arrival node of every line. The system handles a base power of 1 MVA and a base voltage of 12.66 kV.

**Table 1.** IEEE 33-Node System Data.

| System data | | | | | | |
|---|---|---|---|---|---|---|
| **Line** | **Terminal i** | **Terminal J** | **R[Ω]** | **X [Ω]** | $P_L$ **[MW]** | $Q_L$ **[MVAR]** |
| 1 | 801 | 802 | 0,0922 | 0,0470 | 0,100 | 0,060 |
| 2 | 802 | 803 | 0,4930 | 0,2511 | 0,090 | 0,040 |
| 3 | 803 | 804 | 0,3660 | 0,1864 | 0,120 | 0,080 |
| 4 | 804 | 805 | 0,3811 | 0,1941 | 0,060 | 0,030 |
| 5 | 805 | 806 | 0,8190 | 0,7070 | 0,060 | 0,020 |
| 6 | 806 | 807 | 0,1872 | 0,6188 | 0,200 | 0,100 |
| 7 | 807 | 808 | 0,7114 | 0,2351 | 0,200 | 0,100 |
| 8 | 808 | 809 | 1,0300 | 0,7400 | 0,060 | 0,020 |
| 9 | 809 | 810 | 1,0440 | 0,7400 | 0,060 | 0,020 |
| 10 | 810 | 811 | 0,1966 | 0,0650 | 0,045 | 0,030 |
| 11 | 811 | 812 | 0,3744 | 0,1238 | 0,060 | 0,035 |
| 12 | 812 | 813 | 1,4680 | 1,1550 | 0,060 | 0,035 |
| 13 | 813 | 814 | 0,5416 | 0,7129 | 0,120 | 0,080 |
| 14 | 814 | 815 | 0,5910 | 0,5260 | 0,060 | 0,010 |
| 15 | 815 | 816 | 0,7463 | 0,5420 | 0,060 | 0,020 |
| 16 | 816 | 817 | 1,2890 | 1,7210 | 0,060 | 0,020 |
| 17 | 817 | 818 | 0,7320 | 0,5740 | 0,090 | 0,040 |
| 18 | 802 | 819 | 0,1640 | 0,1565 | 0,090 | 0,040 |
| 19 | 819 | 820 | 1,5042 | 1,3554 | 0,090 | 0,040 |
| 20 | 820 | 821 | 0,4095 | 0,4784 | 0,090 | 0,040 |
| **System data** | | | | | | |
| **Line** | **Terminal i** | **Terminal J** | **R[Ω]** | **X [Ω]** | $P_L$ **[MW]** | $Q_L$ **[MVAR]** |
| 21 | 821 | 822 | 0,7089 | 0,9373 | 0,090 | 0,040 |
| 22 | 803 | 823 | 0,4512 | 0,3083 | 0,090 | 0,050 |
| 23 | 823 | 824 | 0,8980 | 0,7091 | 0,420 | 0,200 |
| 24 | 824 | 825 | 0,8960 | 0,7011 | 0,420 | 0,200 |
| 25 | 806 | 826 | 0,2030 | 0,1034 | 0,060 | 0,025 |

**Table 2.** (Continued): IEEE 33-Node System Data.

| | | | | | | |
|---|---|---|---|---|---|---|
| 26 | 826 | 827 | 0,2842 | 0,1447 | 0,060 | 0,025 |
| 27 | 827 | 828 | 1,0590 | 0,9337 | 0,060 | 0,020 |
| 28 | 828 | 829 | 0,8042 | 0,7006 | 0,120 | 0,070 |
| 29 | 829 | 830 | 0,5075 | 0,2585 | 0,200 | 0,600 |
| 30 | 830 | 831 | 0,9744 | 0,9630 | 0,150 | 0,070 |
| 31 | 831 | 832 | 0,3105 | 0,3619 | 0,210 | 0,100 |
| 32 | 832 | 833 | 0,3410 | 0,5302 | 0,060 | 0,040 |

## 3 Selecting the optimal dimensioning for distributed generation

For the dimensioning of the distributed generation units, the method stated in [1] is used. In this method, the effective power (both active and reactive) delivered by the node is determined, i.e., it not only includes the loads connected to the node but the entire demand beneath it.

The formulation stated in [1] is based in Figure 2. Once the effective power in every node is found, the corresponding losses can be determined using equation (1) without having any generation source connected to the nodes.

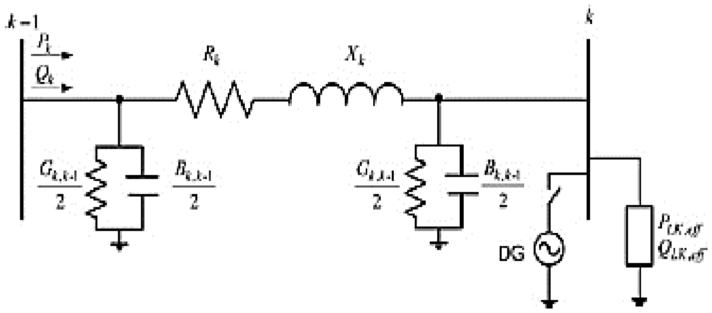


**Figure 2**. Simple Radial System with Feeder

$$P_L^- = \frac{(P_{Lk,eff}^2 + Q_{Lk,eff}^2)}{|V_k^2|} \tag{1}$$

Once the distributed generation has been installed in bus *k*, the losses in the path between *k* and *k-1* can be estimated by (2):

$$P_L^+ = \left[\frac{(P_{DG} - P_{Lk,eff})^2}{|V_k^2|} + \frac{(Q_{DG} - Q_{Lk,eff})^2}{|V_k^2|}\right] \times R_k \tag{2}$$

The difference between the power losses before and after the installation of the DG in node *k* is given by:

$$\Delta P_L = P_L^+ - P_L^- \tag{3}$$

By expanding (4):

$$\Delta P_L = \left[\frac{P_{DG}^2 + Q_{DG}^2 - 2P_{DG}\,P_{Lkeff} - 2Q_{DG}Q_{Lkeff}}{|V_k^2|}\right] xR_k \tag{4}$$

With the purpose of minimizing power losses from the source to section *k*, *k-1*, (4) is derived in terms of the power injected by the DG unit and is equaled to zero.

$$\frac{\partial \Delta P_L}{\partial P_{DG}} = 0 \tag{5}$$

After derivation, the optimal DG value is obtained as in (6):

$$S_{DG} = \sqrt{(P_{DG}^2 + Q_{DG}^2)} \tag{6}$$

Additionally, the dimensioning of the distributed generation in Watts is given by equation (7)

$$P_{DG} = \frac{P_{Lk,eff} + \alpha Q_{Lk,eff}}{1 + \alpha^2} \tag{7}$$

The reactive power in VAR is defined by (8):

$$Q_{DG} = \frac{P_{Lk,eff} + \alpha Q_{Lk,eff}}{\alpha + \beta} \tag{8}$$

Here

$$\alpha = \tan\theta = \frac{Q_{DG}}{P_{DG}} \tag{9}$$

$$\beta = \cot\theta = \frac{P_{DG}}{Q_{DG}} \tag{10}$$

and Θ is the angle of the power factor of the DG.

## 4 Methodology and algorithm developed in python

The 33-node IEEE case study has a radial network that allows the application of the analytical method to be implemented.

The calculation program PowerFactory, developed by DigSILENT, is a computer-assisted Engineering tool for the analysis of transmission, distribution and electrical energy systems. It has been designed as an advanced software package integrated and interactive which is dedicated to the analysis of control and electrical energy systems to reach the main goals of optimization, planning and operation [5]. Python is an independent object-oriented scripting platform language that can build any program from Windows applications to network servers and even websites. It is an interpreted language which means that the code does not need to be compiled in order to be executed which offers advantages such as a fast development speed and disadvantages such as a lower speed [5]. The communication between DigSilent and Python was implemented using a source code script written in IDLE (Python GUI) and executed in DigSilent. The source code has four functions:

a. Load flow( ) function: This function is in charge of executing the load flow with the purpose of obtaining the data of every element that is a part of the system and executing the algorithm indicated in [1].
b. Disable Events ( ) function: This function basically disables the short-circuit events and switching events of the project that is being studied in DigSilent.
c. Rested( ) function: In order to execute the source code and not generate errors it is necessary to install it in every node except for the DG generation units so that they do not affect the initial conditions for the calculations. This function shows as zero the DG power and the power factor.
d. Size_GD( ) function: Inside this function is found the most relevant part of the code since it executes the algorithm defined in [1] and the data on the screen.

In this work, the optimal dimensioning and location of the DG unit are implemented using the equations (8), (9), (10) and (11). For this testing system, the maximum real power's limit is supposed to be equal to the system load's total real power. Hence, a maximum number of DG units is considered as [1].

The algorithm to locate the DG unit in the IEEE radial system of 33 nodes is the following:

1. Read the data from the load flow for the base case.
2. Compute $P_{Lk,eff}$ y $Q_{Lk,eff}$ using:

$$P_{lkeff} = \sum_{i=n}^{NB} P_{L_i} + \sum_{i=n}^{NB-1} P_{Lossk} \tag{12}$$

$$Q_{lkeff} = \sum_{i=n}^{NB} Q_{L_i} + \sum_{i=n}^{NB-1} Q_{Lossk} \quad (13)$$

Here:

$P_{Lk,eff}$: Total active power load fed by bus *n* in the case study.
$Q_{Lk,eff}$: Total reactive power load fed by bus *n* in the case study.
$P_{Lossk}$: Active power losses between the lines that unite the nodes *k* and *k-1* in the case study.
$Q_{Lossk}$ : Reactive power losses between the lines that unite the nodes *k* and *k-1* in the case study.

3. Calculate the dimension of the distributed generation in each node using (8), (9), (10) y (11).
4. Put every dimensioned DG within the nodes of the case study and calculate the active and reactive power losses and the respective voltages of the nodes in the branch of interest.
5. Show on the screen the results collected in step 3.
6. Print the results.

## 5 Results from the case study

When executing the load flow of the 33-node IEEE radial system in the DigSilent software, without the incorporation of the distributed generation, the data shown in table 2 are obtained:

**Table 3.** Results from the load flow of the 33-node IEEE system without DG

| **Active power losses** | **Reactive power losses** | **Minimum power** | **Maximum power** |
|---|---|---|---|
| **MW** | **MVAR** | **Per unit** | **Per unit** |
| 0,202434 | 0,134579 | 0,91329 @ 818 | 1,00 @ 801 |

Once the algorithm has been executed with the Python program, the system nodes with the lower reactive power losses are identified as shown in Table 3 where the nodes 806 and 828 have the lowest losses with 2.59 MVA and 1.20 MVA respectively after the DG units have been implemented in the system (see Table 3).

**Table 4**. Dimensioning of DG unit and power losses

| **Node** | **Dimension of DG [MVA]** | $P_{Loss}$[**MW**] | $Q_{Loss}$[**MVAR**] |
|---|---|---|---|
| 802 | 4,5975 | 0,1889 | 0,1275 |
| 803 | 4,0312 | 0,1335 | 0,0983 |
| 804 | 2,8719 | 0,1193 | 0,0910 |
| 805 | 2,7069 | 0,1018 | 0,0816 |
| 806 | 2,5902 | 0,0649 | 0,0497 |
| 807 | 1,1666 | 0,1117 | 0,0733 |
| 808 | 0,9761 | 0,1181 | 0,0787 |
| 809 | 0,7483 | 0,1291 | 0,0855 |
| 810 | 0,6824 | 0,1304 | 0,0861 |
| 811 | 0,6203 | 0,1347 | 0,0892 |
| 812 | 0,5654 | 0,1384 | 0,0919 |
| 813 | 0,4926 | 0,1421 | 0,0940 |
| 814 | 0,4222 | 0,1482 | 0,0976 |
| 815 | 0,2776 | 0,1636 | 0,1079 |
| 816 | 0,2210 | 0,1703 | 0,1124 |
| 817 | 0,1591 | 0,1782 | 0,1177 |
| 818 | 0,0976 | 0,1869 | 0,1237 |
| 819 | 0,3916 | 0,2002 | 0,1333 |
| 820 | 0,2929 | 0,1999 | 0,1329 |
| 821 | 0,1952 | 0,2004 | 0,1331 |
| 822 | 0,0976 | 0,2012 | 0,1337 |
| 823 | 1,0357 | 0,1694 | 0,1169 |
| 824 | 0,9263 | 0,1669 | 0,1143 |
| 825 | 0,4624 | 0,1805 | 0,1215 |
| 826 | 1,3544 | 0,1011 | 0,0716 |
| 827 | 1,2863 | 0,1012 | 0,0719 |
| 828 | 1,2064 | 0,0940 | 0,0647 |
| 829 | 1,0216 | 0,0987 | 0,0662 |
| 830 | 0,9559 | 0,0997 | 0,0672 |
| 831 | 0,4678 | 0,1406 | 0,0931 |
| 832 | 0,3032 | 0,1594 | 0,1054 |
| 833 | 0,0721 | 0,1912 | 0,1269 |

Figure 3 shows the relation between the size of the DG unit and the system losses with that specific dimension.

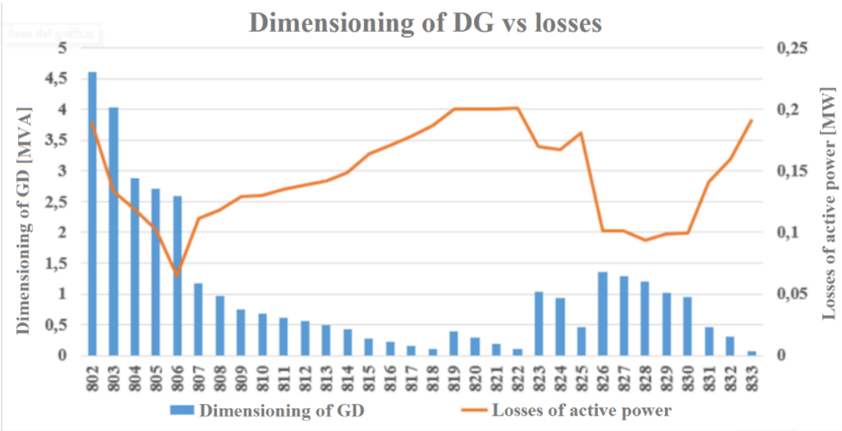


**Figure 3.** DG dimensioning versus losses

**Table 5.** Optimal location and size of DG units

| Optimal location | Dimension DG [MVA] | Losses [MW] | % Reduction of losses |
|---|---|---|---|
| 806 | 2.5902 | 0,0649 | 67,87% |
| 828 | 1.2064 | 0.0940 | 53,46% |

For seeing the consequence overload voltage profiles in the studied system, at the first DG is located in the node with lowest losses within system which is node 806; once this has been performed, the load flow is executed and the voltage data from the nodes in p.u. are registered. The same task is carried out with the following DG where the node would be 828 as seen in Table 4.

To further observe the behavior of the voltage without DG, with one DG and with two DGs, the Figure 4 is plotted with its values detailed in Table 5.

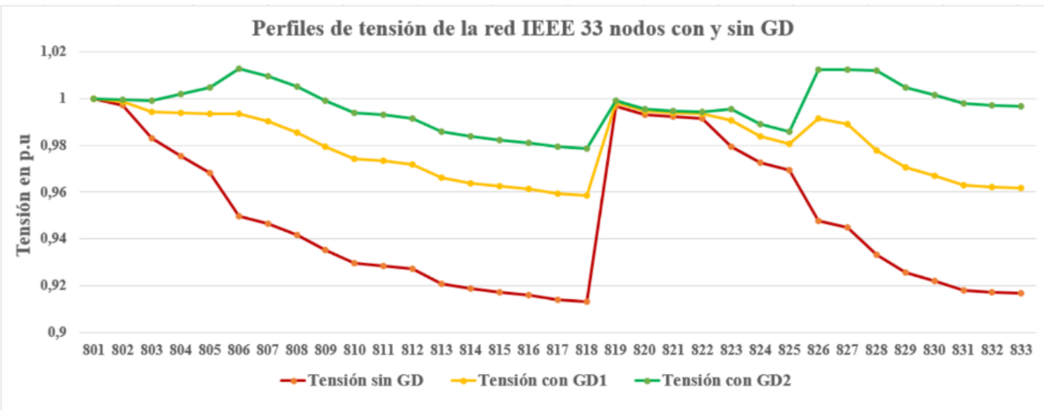


**Figure 4.** Voltage profiles in the 33-node IEEE system in three scenarios: without DG (**red**), with one DG (**yellow**) and two DG (**green**)

**Table 5.** Voltage profiles with and without DG (given in p.u.)

| Node | Without GD | With GD1 | With GD2 |
|---|---|---|---|
| 801 | 1,0000000 | 1,0000000 | 1,0000000 |
| 802 | 0,9970333 | 0,9988032 | 0,9995841 |
| 803 | 0,9829445 | 0,9941720 | 0,9991263 |
| 804 | 0,9754669 | 0,9936801 | 1,0017180 |
| 805 | 0,9680738 | 0,9935528 | 1,0047970 |
| 806 | 0,9496837 | 0,9933888 | 1,0126760 |
| 807 | 0,9463539 | 0,9902119 | 1,0095620 |
| 808 | 0,9415122 | 0,9855920 | 1,0050340 |
| 809 | 0,9352481 | 0,9796177 | 0,9991798 |
| 810 | 0,9294374 | 0,9740763 | 0,9937500 |
| 811 | 0,9285775 | 0,9732563 | 0,9929464 |
| 812 | 0,9270790 | 0,9718274 | 0,9915464 |
| 813 | 0,9209708 | 0,9660041 | 0,9858410 |
| 814 | 0,9187059 | 0,9638449 | 0,9837256 |
| 815 | 0,9172950 | 0,9625000 | 0,9824080 |
| 816 | 0,9159300 | 0,9611989 | 0,9811334 |
| 817 | 0,9139047 | 0,9592684 | 0,9792422 |
| 818 | 0,9132981 | 0,9586903 | 0,9786759 |
| 819 | 0,9965049 | 0,9982757 | 0,9990571 |
| 820 | 0,9929273 | 0,9947045 | 0,9954887 |
| 821 | 0,9922228 | 0,9940012 | 0,9947860 |
| 822 | 0,9915853 | 0,9933650 | 0,9941502 |
| 823 | 0,9793590 | 0,9906278 | 0,9956001 |
| 824 | 0,9726881 | 0,9840339 | 0,9890397 |
| 825 | 0,9693636 | 0,9807479 | 0,9857704 |
| 826 | 0,9477011 | 0,9914976 | 1,0125270 |
| 827 | 0,9450636 | 0,9889819 | 1,0124480 |
| 828 | 0,9332725 | 0,9777354 | 1,0118840 |
| 829 | 0,9256202 | 0,9704377 | 1,0048390 |
| 830 | 0,9220656 | 0,9670478 | 1,0015660 |
| 831 | 0,9179070 | 0,9630829 | 0,9977389 |
| 832 | 0,9169921 | 0,9622107 | 0,9968970 |
| 833 | 0,9167086 | 0,9619404 | 0,9966361 |

## 6 Analysis of Results

With the results obtained with the implementation of the program led to determine that the nodes 806 and 828 are optimal for the DG connection with a reduction of power losses that coincides with [1].

The voltage profiles (Figure 4) evidently improve which translates into a reduction of the voltage drops. This simulation presents the same behavior pattern of [3].

**Table 6.** Improvement of voltage profile in node 818

| **Node** | **Voltage** | | |
|---|---|---|---|
| | **Without DG** | **DG1** | **DG2** |
| 818 | 0,9132981 | 0,9586903 | 0,9786759 |

The variation of the results after executing the program in Python and DigSilent lies in the topology and specification of the power system taken as a case study. Although the 33-node IEEE system detailed in [8] is used as a reference, it does not guarantee that the system does not present changes in the executions of the references work. Additionally, the calculations of the used references are based on approximate data and the program designed in Python takes the exact values of the line losses and the power demanded in the system terminals.

**Table 7.** Data comparison – Python VS theoretical reference

| **Location** | **DG Dimension [MVA]** | | **Losses[MW]** | |
|---|---|---|---|---|
| **Optimal** | **Python** | **Analytical [1]** | **Python** | **Analytical [1]** |
| 806 | 2,5902 | 2,48 | 0,0649 | 0,069 |
| 828 | 1,2064 | 1,204 | 0,094 | 0,056 |

The 80@ assignment is meant only to facilitate the recognition of nodes within the system: for [1] the node 6 is the node 806 as the node 28 of [1] is node 828 in the present work.
To select the power factor of the generation unit, the one stated in [2] is used which has a value of 0.85 in delay.

## 7 Conclusions

The tests carried out with the proposed algorithm show how the optimal location of the DG within the network facilitates the reduction of losses. For the specific case, the levels reached 67.87% in the nodes where the algorithm showed the optimal location of the DG.

The variations in the voltage profiles show changes lower than 5% for the scenarios including DG1and DG2. This is valid both for the nodes where the DG were located as for the ones it affected indirectly.

The incorporation of distributed generation reduces the system's power losses. This can be explained to an increase in the voltage levels once the DG unit (or units) is installed which lowers the current necessary to supply the power requirements. Hence, the current that circulates through the lines is lower translating into a reduction of losses.

## References

[1] A. M. Abd-el-Motaleb and S. K. Bekdach, Optimal sizing of distributed generation considering uncertainties in a hybrid power system, *Int. J. Electr. Power Energy Syst.*, **82** (2016), 179–188. https://doi.org/10.1016/j.ijepes.2016.03.023

[2] A. Bagheri, H. Monsef and H. Lesani, Integrated distribution network expansion planning incorporating distributed generation considering uncertainties, reliability, and operational conditions, *Int. J. Electr. Power Energy Syst.*, **73** (2015), 56–70. https://doi.org/10.1016/j.ijepes.2015.03.010

[3] P. Chiradeja and A. Ngaopitakkul, The impacts of electrical power losses due to distributed generation integration to distribution system, *2013 Int. Conf. Electr. Mach. Syst. ICEMS*, (2013), 1330–1333. https://doi.org/10.1109/icems.2013.6713271

[4] S. Elsaiah, M. Benidris and J. Mitra, An analytical method for placement and sizing of distributed generation on distribution systems, *2014 Clemson Univ. Power Syst. Conf.*, **7** (2016), 1–7. https://doi.org/10.1109/psc.2014.6808097

[5] R. H. Lasseter, Microgrids and Distributed Generation, *J. Energy Eng.*, **133** (2007), no. 3, 144–149. https://doi.org/10.1061/(asce)0733-9402(2007)133:3(144)

[6] A. Rujula, J. Amada and J. Bernal-Agustin, Definitions for Distributed Generation: A Revision, *International Conf. Renew. Energy Power Qual.*, (2005), 16–18.

[7] H. Tazvinga, X. Xia and B. Zhu, Optimal energy management strategy for distributed energy resources, *Energy Procedia*, **61** (2014), 1331–1334. https://doi.org/10.1016/j.egypro.2014.11.1093

[8] Y. Yuan, Z. Wei, G. Sun, Y. Sun and D. Wang, A real-time optimal generation cost control method for virtual power plant, *Neurocomputing*, **143** (2014), 322–330. https://doi.org/10.1016/j.neucom.2014.05.060

**Received: September 26, 2017; Published: November 8, 2017**